OPTIMUM MULTI-TARGET DETECTION USING AN ANC NEURO-FUZZY SCHEME AND WIDEBAND REPLICA CORRELATOR

Chien-Hsun Tseng and Marina Cole

School of Engineering, University of Warwick, UK

ABSTRACT

An optimum target detection algorithm is developed for underwater active wideband sonar signal in the presence of reverberation and ambient noise. The hybrid algorithm makes use of an adaptive ANC neuro-fuzzy scheme in the first instance to provide an effective fine tuned signal followed by an iterative cross correlation-based target motion estimation (TME) scheme for efficient target detection. Computer simulations based on real input data sets demonstrate capability and efficiency of the proposed hybrid algorithm in extracting even zero-Doppler target signals from a highly reverberated noisy environment.

***Index Terms*—** echolocation, reverberation, ANC, ANFIS, wavelets, optimal wideband replica correlator.

1. INTRODUCTION

Let us consider the underwater returns with reflected wideband target signals against a background interference involving reverberations and ambient noise. The mathematical model of the backscattered signal in a nondirectional sonar channel can be described as [1]

$$\tilde{g}(t) = \sum_{i=1}^{I} \alpha_i g_i(t) + \eta(t) \tag{1.1}$$

where the wideband target signatures $g_i(t)$ associated with echo attenuation value α_i are received as Doppler distorted pulses at time $t \in \Omega \subset \Re$ in the Hilbert Space of finite energy signals $L^2(\Omega)$, and the interference $\eta(t)$ involves a reverberation waveform $r(t)$ and additive ambient noise $n(t)$:

$$g_i(t) = \sqrt{S_i}\psi(S_i(t - D_i)), \eta(t) = \hbar(t) * r(t) + n(t) \tag{1.2}$$

Here ψ denotes the transmitted signal, S_i and D_i represent the true Doppler scale and two-way time-shift of the i^{th} echo, respectively, and $\hbar$ is an unknown arbitrary noise path filter convoluted with the reverberation pulses to further complicate the scattered returns. Reverberations due to multiple reflection from the medium boundaries including the surface, volume and bottom usually contribute in varying proportions. With the scenario chosen for which the sonar devices are assumed to be mounted on a surface ship, the scattering process and the dependence of the received reverberation on range can be modelled in terms of having an intensity with exponential statistics or an envelope, a square root of the intensity, with the Rayleigh statistic. The probability density function of the reverberation model distributed by the Rayleigh statistics is then given by $\wp(\gamma|\sigma) = \frac{\gamma}{\sigma^2} e^{-\gamma^2/2\sigma^2}$ where γ is the amplitude of the envelope and σ is the standard deviation representing the expected level of intensity.

The aim of the model in Eqs. (1.1-1.2) is to isolate specular returns from the background interference. Hence, a pair of scale-time joint motion parameters $(\hat{S}_i, \hat{D}_i)$ associated with the i^{th} return can then be estimated. Technique used to measure the scale-time of objects is commonly known as the wideband cross correlation or matched filter processing [2]. The wideband cross correlation processing works well and has optimum performance with the maximum output of target strength [3]. In the presence of severe interference including reverberation and ambient noise, an ANC neuro-fuzzy scheme powered by ANFIS [4, 5] processor has offered a possible remedy to effectively remove unwanted noise. The stage of noise cancelling exploits capabilities of ANFIS in tracking both linearity and nonlinearity between signal and interference/noise, and hence improves the target strength. More recently, an iterative CWT-based TME scheme [5] was incorporated with the ANC neuro-fuzzy scheme to yield a complete hybrid algorithm. CWT-based TME scheme proposed was not only to effectively localize and identify targets, but also as a step towards an efficient hardware implementation. Due to sidelobe correlation occurred at the CWT mapping, an alternative cross correlation-based TME scheme consisted of rimmed mean (TM)-levelization, discrete wavelet denoising (WDeN), and the optimal wideband replica correlator (WRC) is proposed to alleviate the sidelobe correlation interference [6] and thus increase accuracy of the target detection in terms of motion parameters estimation. Simulation results based on real input data sets show that with a little help from the ANC neuro-fuzzy scheme in the first instance, the proposed cross correlation-based TME scheme is effective and cost-efficient in recovering even zero-Doppler with very low echoes from a highly reverberated noise environment.

THIS WORK IS SUPPORTED BY EPSRC(UK) AND MOD(UK) JOINT PROJECT UNDER GRANT NO. GR/T12262101.

2. OPTIMAL WIDEBAND CORRELATION PROCESS

2.1. Wideband correlation

Having a system model in Eq. (1.1), a point target return can be described as a wideband cross ambiguity function [2]:

$$WC_{\psi\tilde{g}}(s, \tau) = \int_{-\infty}^{\infty} \tilde{g}(t)\overline{\psi_s(t - \tau)}dt \tag{2.1}$$

where $\psi_s(t) \equiv \sqrt{s}\psi(st)$ constituting the form of a hypothetical signal with a Doppler scale s is a template. Eq. (2.1) sometimes is referred to as wideband matched filter or WRC, and the standard cross correlation estimator maximizes the magnitude squared of the WRC for detection of known waveforms of unknown complex amplitude and unknown time of arrival (TOA) of targets distorted by background interferences. If the incoming signal receives maximum output target strength in terms of SNR and $\eta(t)$ is an additive white Gaussian noise of known variance, the correlation process is optimum [3]. Assume that the transmitted signal $\psi(t)$ is completely specified and characterized by a modulation function $\mathbf{m}(t)$ having a unity power within an envelope $w(t)$, i.e.,

$$\psi(t) = w(t)\mathbf{m}(t), \text{ subject to } ||\mathbf{m}(t)||^2 = 1. \tag{2.2}$$

Since the statistic of WRC is tested against a threshold for the presence of a received complex echo and the local maximum is an estimate of the TOA, the WRC detection can be solved by equivalently seeking a local maximum of the RC output with respect to $w(t)$ over both parameters simultaneously:

$$\max_{s>0,\tau\in\Omega}\{|WC_{\psi\tilde{g}}(s,\tau)|^2\} = |WC_{w\tilde{g}}(s^*,\tau^*)|^2$$

where (s^*,τ^*) is a pair of local maximizer. Since s^* in the correlation process is proportional to the true scale, one can accordingly obtain the desired parameters $\hat{S} = s^*/\varepsilon, \varepsilon > 0$ and $\hat{D} = \tau^*$ as estimates of S and D, respectively. Consequently, the echolocation single point target detection may be solved by seeking a local maximum of the continuous time-scale joint representation:

$$\max_{s>0,\tau\in\Omega}\{|WC_{w\tilde{g}}(s,\tau)|^2\}. \quad (2.3)$$

The above single point target problem can be extended to a multi-target one, which can be written as a multi-dimensional semi-infinite quadratic programming problem:

$$\begin{array}{ll} \max & \mathbf{f}(\mathbf{s},t) = \sum_{i=1}^{m} |WC_{w\tilde{g}}(s_i,\tau(t))|^2 \\ \text{subject to} & \mathbf{s}(t) > 0_m, \forall t \in \Omega. \end{array}$$

where $\mathbf{s} \equiv [s_1,\ldots,s_m]' \in \Re^m$ denotes a vector form of m-target Doppler scales.

Remark 2.1

- *The detection process in time domain through Eq. (2.3) is independent of $\mathbf{m}(t)$, which is modulated by a carrier frequency. This advantage makes it easier to implement digitally as only the window function (a lowpass waveform) needs to be sampled. In contrast, the carrier frequency in frequency domain cannot be separated from the window function due to the wideband condition [2].*
- *By defining the unity modulated signal in Eq. (2.2), the WRC employs only the mainlobe of the replica. This has alleviated the sidelobe correlation interference problem [6] in which strong, near-specular unwanted harmonics of the transmission entering the mainlobe correlating with the unmodulated replica.*

2.2. Discrete mapping of the WRC

We will require a discrete-time version of Eq. (2.3) for digital implementation. The discrete-time equivalent of the WRC can be processed through matched filtering in the sequence space ℓ^2 as follows:

$$\begin{aligned} WC_{w\tilde{g}}(s,\tau) &= \sqrt{s}\int_{-\infty}^{\infty}\tilde{g}(\tau+t)\overline{w(st)}dt \\ &= \sqrt{s}\sum_l\int_{\ell}^{l+1}\tilde{g}(\tau+t)\overline{w(st)}dt. \end{aligned} \quad (2.4)$$

Let $\tilde{g}(t) = \tilde{g}(l) \in \ell^2$ for all $t \in [l, l+1]$. Eq. (2.4) can be approximated as

$$\begin{aligned} WC_{\psi\tilde{g}}(s,\tau) &\approx \sqrt{s}\sum_l\tilde{g}(\tau+l)\int_{\ell}^{l+1}\overline{w(st)}dt \\ = \tfrac{1}{\sqrt{s}}\sum_l\tilde{g}(\tau+l)\int_{sl}^{s(l+1)}\overline{w(t)}dt &= \sum_l\tilde{g}(\tau+l)M(s,l). \end{aligned}$$

Provided an effective support $t \in [-T_w, T_w]$ for $w(t)$ with the sampling rate f_w, the discrete indices l are bounded within $\frac{[-T_w/s, T_w/s]}{2T_w/s}(2T_w f_w - 1)$ and the matched filter $M(s,l)$ can be obtained:

$$M(s,l) = \tfrac{1}{\sqrt{s}}\left[\int_{-\infty}^{s(l+1)}\overline{w(t)}dt - \int_{-\infty}^{sl}\overline{w(t)}dt\right]. \quad (2.5)$$

Now let us consider Eq. (2.3) with support $t \in [0,T]$. The discrete-time version of the problem following from Eq. (2.5) consists of breaking the time interval $[0,T]$ into N subintervals, and approximating the input signal $\tilde{g} \equiv [\tilde{g}(0),\ldots,\tilde{g}(N-1)]$. The correlation coefficient obtained for the $(k+1)$-th input signal, $\tilde{g}(k)$ is then expressed by an output response with coefficients $h(s,k)$ at the scale s , i.e.,

$$WC_{w\tilde{g}}[s,k] = y[s,k] = \sum_{\ell=0}^{N-k-1}\tilde{g}(s,k+\ell)M(\ell) \quad (2.6)$$

for $k = 0,\ldots,2N-2$. Due to the discrete setting in the time-domain, the target detection in the continuous time-scale joint setting of Eq. (2.3) is reduced to a semi-infinite scale setting problem. Consequently, the problem of seeking a pair of optimizer (s^*,τ^*) may be solved by the following algorithm:

Algorithm 2.1 *[7] Set $i = 1$. Let $f(s) \equiv \sum_{k=0}^{N-1}|\hat{y}[s,k]|^2$, where $\hat{y}[s,k] = \hat{g}(k)oM(s,k)$ and $\hat{g}$ is a denoised signal of $\tilde{g}$. Denote $f^n(s), n = 1,2,\ldots$ by the n-th derivative of $f(s)$. Define $\epsilon > 0$ and Doppler scales s_0, s_{min}, s_{max} which represent the stationary, minimum and maximum target motions, respectively with their corresponding time indices k_0, k_{min}, k_{max}.*

1. *Find an optimizer $\hat{s}_i^*$ that maximizes $f(s)$, i.e., $\hat{s}_i^* = arg\max_{s>0} f(s)$.*
2. *Provided the scale $\hat{s}_i^*$, the corresponding time-delays $\hat{\tau}_{i,j}^{*n} = \hat{\tau}_i^*(k_j^n), j = 1,2\ldots$ can be obtained for which indices k_j^n are given by*
$$k_j^n = arg\max_k\{|f^n(\hat{s}_i^*) - f(\hat{s}_i^*)|\}. \quad (2.7)$$
3. *If the stopping criteria*
$$\frac{|k_j^n - k_0|}{\max\{|k_{min}-k_0|,|k_{max}-k_0|\}} < 1, |k_j^n - k_j^{n-1}| \le \epsilon$$
are satisfied, then stop and set $(s^*,\tau^*) = (\hat{s}_i^*, \hat{\tau}_i^*(k_j^n))$; otherwise return to Step 1. with index i replaced by $i+1$.

3. HYBRID ALGORITHM AND COMPUTER SIMULATIONS

Depicted by Fig. 1, the proposed hybrid algorithm includes two schemes: ANC neuro-fuzzy scheme in Fig. 1(a) and cross correlation-based TME scheme in Fig. 1(b).

3.1. ANC neuro-fuzzy scheme

The adaptive ANC neuro-fuzzy scheme consists of a primary input channel corrupted by two types of interference: η_{r_n} and η_n in the reference channel and is processed by the adaptive neuro-fuzzy inference systems (ANFIS). In particular, two unknown systems with noise path filters, $\hbar_1$ and $\hbar_2$ are applied as parts of the scattered return adding together with the contact signal to form the primary channel. For simplicity, the noise path filters are chosen to be characterized by linear/nonlinear functions with two reference inputs x_1 and x_2:

$$\hbar_1(x_1,x_2) = 20(x_1+x_2)+5$$
$$\hbar_2(x_1,x_2) = 100(x_2-x_1^2)^2 + (1-x_1)^2.$$

For the ANFIS model, the input data training set is received from the reference channel formed by combination of reverberation signal and ambient noise. Given membership functions (MFs) on each inputs, the ANFIS operation adaptively localize the nonlinear relationships among η, $\mathbf{r}$, and $\mathbf{n}$, thus, produces an estimate $\hat{\eta}(t)$ in the output. The noise data contained in the high frequency ranges of the input signal is then subtracted and thus yielded an estimated output.

3.2. TME scheme

Provided the denoised signal as source of input, the iterative TME scheme is devoted to further noise suppression and final target identification for which potentials reside in a very low frequency. The TME scheme is comprised of three processes:

- TM-levelization: Its functionality is to generate dynamic level-based step-sizes to keep updating the TME scheme. As the process slides through the ANC neuro-fuzzy output, two dynamic gauges TM_{α_1} and TM_{α_2} are introduced at different level to achieve fast convergence by removing power of most of the sharp detail information in the sense of trimmed mean estimation.

- WDeN: This operation is associated with an octave sub-band decomposition designed to further suppress the noise part of the training data by using thresholding rule to the detail coefficients. The denoising operation is proven to be efficient as can be viewed as a nonparametric estimation of the noise-free desired signal [9].

- Optimal WRC: This function is to resolve the discrete-time version of Eq. (2.3) by going through Algorithm 2.1 iteratively. In particular, one needs to solve a constrained optimization problem with continuous nonlinear objective function of the Doppler scale s in Step 1. Instead of discretising the continuous-scale using a sampling rate sufficiently high to capture enough information for approximating the optimal solution, the nonlinear optimization problem can be solved by a combination of golden section search and successive parabolic interpolation method [10].

3.3. Processing results

We test the hybrid algorithm for underwater multiple target detection using real sonar data sets based on Morlet wavelet as the signal source for target echoes and reverberation waveform. For each ping, the source sweeping continuously over a $2ms$ long transmission interval of 1 second amid the following environment settings: sea depth (=100m), sonar depth (=50m), wind speed (=6m/s $\sim$ sea state 3), seabed type (=medium sand), target range (=500m). Two synthetic discrete contact signals g_{T_1} and g_{T_2} with details described in Table 1 were added to the background interference shown in Fig. 2(a) with TOA of T_1 and T_2 marked with circular character. The interference containing reverberation waveform $r(t)$ and white Gaussian noise $n(t)$ with $WGN(0, 0.25)$ are sampled at $f_s = 100kHz$ and depicted in Fig. 2(b). The composite ANC primary input signal with the echo strength of SNR = -30dB is shown in Fig. 2(c). More specifically, the interference waveform is a result of four-channel outputs going through two unknown noise path filters. These channels including two reverberation channels and two ambient noise channels process data to collect totally $N = 100k$ input-output data pairs in the fuzzy inference system for predicting the behavior of the unknown nonlinear noise path filters. Among them 50% of the data set is taken for the training nodes, and 50% of the others is for checking modes to validate the fuzzy model. Provided two Gaussian MFs on each of the four-channel reference outputs, patterns of noise residing in the high frequency ranges were estimated involving 8 epoches of ANFIS operation leading the output of the ANC neuro-fuzzy scheme to an estimated signal for identifying T_1 of the contact signal g_{T_1}. As compared with the composite signal in Fig. 2(c), Fig. 3(a) shows that most of the noisy signal have been removed leaving the signal at hand contains sufficient information ready to proceed in the TME scheme. Passing the data through the TM-levelization process with setting $TM_{\alpha_1} = TM_{\alpha_2} = 0$, noise in the low frequency ranges is further suppressed by the WDeN process whose output is depicted in Fig. 3(b). By setting up parameters described in Table 1 for the replica function $w(t)$, Fig. 3(c) shows the the resultant signal of Eq. (2.7) with the order $n = 2$, i.e., the 1^{st} iteration of the TME scheme with an estimated location T_{1e} marked with diamond character. Clearly, the optimal WRC process fails to resolve the T_1 marked with circle character. Increasing the TM level by $TM_{\alpha_1} = TM_{\alpha_2} = 7.5 \times 10^{-4}$ equivalent to removing power of $15.67dB$ down from the peak magnitude of the ANC output following by the WDeN process has yielded more noise being suppressed out of the system as can be viewed in Fig. 3(d). The target detection for T_1 was successfully carried out through the optimal WRC process at the 2^{nd} iteration of TME whose output is shown in Fig. 3(e) where as can be also viewed clearly in Table 2 the estimated location of TOA T_{1e} closely matched to the ideal location T_1. We note that the ideal outputs in Table 2 are given as reference for the purpose of comparison only.

Similar to the detection of T_1, Figs. 4(a)-(e) gives details of detection done for the T_2. More precisely, the ANC output depicted in Fig. 4(a) yields an estimated signal $\hat{g}$ being fine tuned by ANFIS with 8 epoches of operation. Following by the 1^{st} iteration of TME scheme, the denoised signal by the WDeN process is presented in Fig. 4(b) leading to a false alarm T_{2e} and is shown in Fig. 4(c). Increasing the TM level to $TM_{\alpha_1} = TM_{\alpha_2} = 7.5 \times 10^{-4}$ equivalent to $15.64dB$ down from the peak magnitude of the ANC output, Figs. 4(d)-(e) show a successful detection at the 2^{nd} iteration of TME scheme. In particular, the denoised signal in Fig. 4(d) has paved the way for lower linear/nonlinear mapping in the optimal WRC process to arrive at the estimated location T_{2e} in Fig. 4(e) exactly matching the ideal location T_2. Details of the ideal and estimated motion parameters regarding the synthetic echoes g_{T_1} and g_{T_2} are illustrated in Table 2.

4. CONCLUSION

A hybrid algorithm consisting of an adaptive ANC neuro-fuzzy and iterative cross correlation-based TME schemes was developed to obtain a joint estimate of Doppler time-scale for underwater active sonar system. The adaptive ANC scheme was used in the first instance to improve the target strength by effectively removing unwanted noise including sidelobe correlation interference and noise contained in the high frequency ranges. The iterative TME scheme was then employed to further reduce noise and hence estimate a joint Doppler time-scale parameter in an efficient and accurate manner. An illustrative example considering multiple target detection using real sonar data sets was cited at the first time, which demonstrates the capability and efficiency of the proposed algorithm in extracting target signals with a very low echo level.

5. REFERENCES

[1] P. C. Etter, Underwater Acoustic Modeling, E&FN SPON, 1996.

[2] L. G. Weiss, "Wavelets and wideband correlation processing," *IEEE Signal Processing Magazine*, pp. 13-32, 1994.

[3] H. Naparst, "Dense target signal processing," *IEEE Trans. Inform. Theory*, vol. 37, pp. 317-327, 1991.

[4] C. H. Tseng and M. Cole, "Adaptive neuro-fuzzy inference systems for wideband signal recovery in a noise-limited environment," FUZZ-IEEE 2007, pp.757-762. 2007.

[5] C. H. Tseng and M. Cole, "A hybrid algorithm based on neuron-fuzz and wavelet transforms for wideband sonar detection in a reverberation-limited environment," EUSIPCO, pp. 1750-1754, Poznan, Poland, 2007.

[6] D. Alexandrou and C. De. Moustier, "Adaptive noise cancelling applied to sea beam sidelobe interference rejection," *IEEE J. Oceanic Eng.*, vol. 13, 1988.

[7] C. H. Tseng and M. Cole, "Wideband active sonar detection using optimal FIR filtering and adaptive noise cancelling schemes," Technical Report, School of engineering, University of Warwick, July 2008.

[8] M. A. Mansour, B. V. Smith, and J. A. Edwards, "PC-based real-time active sonar simulator," *IEE Proc.-Radar, Sonar Navig.*, vol. 144, pp. 227-233.

[9] D. L. Donoho, "De-Noising by soft-thresholding," IEEE Trans. on Inf. Theory, vol. 41, 3, pp. 613-627, 1995.

[10] R. P. Brent, Algorithms for Minimization without Derivatives, Prentice-Hall, Englewood Cliffs, New Jersey, 1973

Synthetic Echo Setting	TOA Location	T_1	T_2
	Duration (ms)	2	2
	Amplitude (α_i)	0.3	0.5
	SNR (dB)	-30	-30
WRC Setting	Replica Sampling Freq.	0.84656	
	Replica Support	$[-189, 189]$	
	Filter Taps No.	$[300, 420]$	
	Doppler Scale	$[0.9, 1.26]$	

Table 1. Characteristics of synthetic echo and WRC.

Synthetic echo	g_{T_1}		g_{T_2}	
Hybrid Output	Ideal	TME	Ideal	TME
Onset time (s)	0.18	0.17973	0.23	0.23
Velocity (Kn)	-0.1	0.3333	1.0	1.0
Location	18100	18105	23117	23117
Range (m)	135.744	135.781	173.372	173.372

Table 2. Comparison between Ideal outputs and the TME outputs.

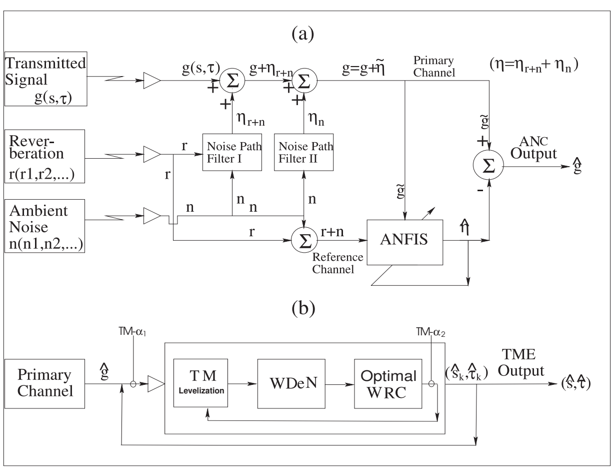

Fig. 1. Adaptive noise cancelling concept for sonar system model.

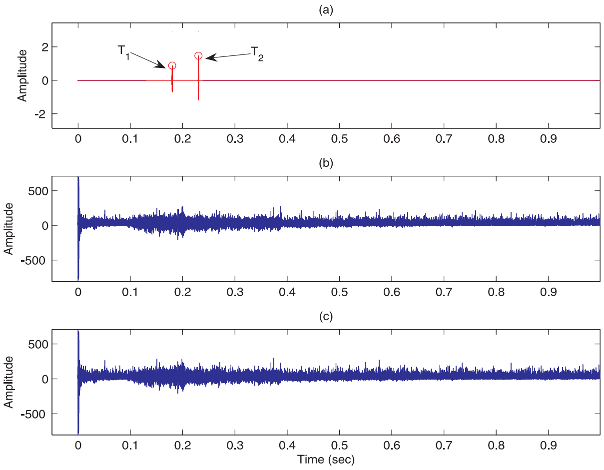

Fig. 2. Time-domain received signals. (a)Noise-free synthetic echoes. (b)Additive interference. (c)Composite returned signal.

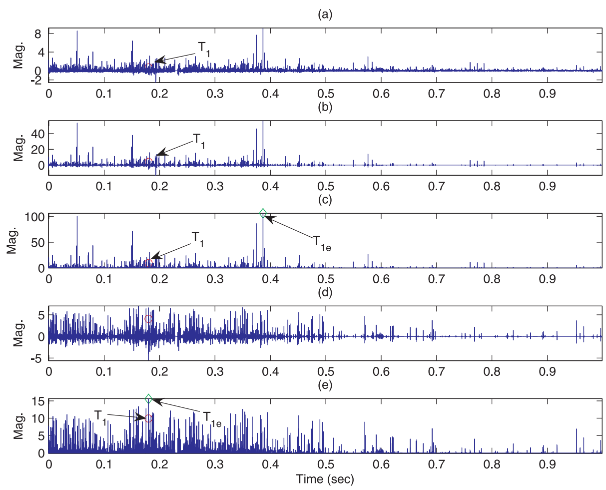

Fig. 3. T_1 detection: (a)ANC neuro-fuzzy output. (b)WDeN output at the 1^{st} iteration of TME. (c)Output of the optimal WRC. (d)WDeN output at the 2^{nd} iteration of TME. (e)Output of the optimal WRC.

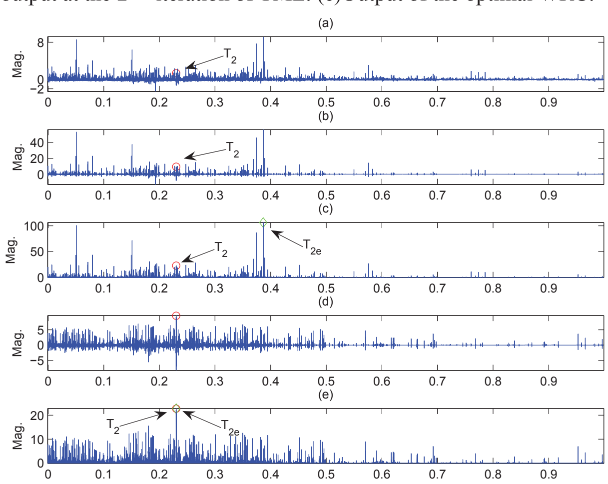

Fig. 4. T_2 detection: (a)ANC neuro-fuzzy output. (b)WDeN output at the 1^{st} iteration of TME. (c)Output of the optimal WRC. (d)WDeN output at the 2^{nd} iteration of TME. (e)Output of the optimal WRC.